

修正 $N-R$ 法과 連續變形法을 이용한 臨界負荷點 및 Nose Curve 算定技法 研究

A Study on the Calculation Scheme of Extreme Loading Point and Nose Curves using Modified $N-R$ and Continuation Method

劉 仁 根*
(In-Keun Yu)

Abstract - Several voltage instability/collapse problems that have occurred in the electric utility industry worldwide have gained the attention of engineers and researchers of electric power systems. This paper proposes an effective calculation scheme of the extreme loading point and nose curves(P-V curves) using modified Newton-Raphson(N-R) load flow method and the Continuation Method. This method provides detail and visual information of the power system voltage profile and operating margin to operators and planners.

In this paper, a modified load flow calculation method for ill-conditioned power systems is introduced for the purpose of seeking more precise load flow solutions and nose curves, and the Continuation Method is also used as a part of the solution algorithm for the calculation of extreme loading point and nose curves. The conventional polar coordinate based N-R load flow program is modified to avoid numerical difficulties caused by the singularity of the Jacobian matrix occurring in the vicinity of extreme loading point of heavily loaded systems. Application results of the proposed method to Klos-Kerner 11-bus system and modified IEEE-30-bus system are presented to assure the usefulness of the approach.

Key Words : Extreme Loading Point(임계부하점), Nose Curve(노우즈 커브),
Continuation Method(연속변형법), Voltage Instability(전압불안정성)

*正 會 員 : 昌原大 工大 電氣工學科 助教授 · 工博
接受日字 : 1992年 3月 4日
1次修正 : 1992年 6月 2日

1. Introduction

The voltage instability/collapse problem has

become one of the most important problems to be solved urgently in major transmission networks planning and operation of modern bulk power systems. A system enters a state of voltage instability when a disturbance, increase in load, or system change causes voltage to drop quickly or drift downward, and operators and automatic system controls fail to halt the decay. Moreover if the decay continues unabated, steady-state angular instability or voltage collapse will occur.

To date, a number of voltage instability/collapse incidents have been reported from the electric power utilities worldwide. The voltage instability phenomenon is not new to power system practising engineers and researchers and the phenomenon was well recognized in radial distribution systems. It was not, however, a problem that transmission planners or system operators had to deal with extensively until recently. It is clear that much of the voltage collapse phenomena is driven by the load rather than the generators, that is, it is recognized that voltage instability and collapse are associated with relatively slow variations in load, network and control characteristics. According to some reports on voltage collapse causing blackouts, frequency and voltage phase angles evidently did not change appreciably. The collapse process therefore may be regarded as being steady-state, rather than transient.

While the basic phenomenon as applied to a radial feeder is well understood and formulated, it is not as simple in a large network. This presents major challenges in establishing sound and simple analytical procedures, quantitative measures of proximity to voltage instability, and adequate operating margins. In recent years, many researchers from electric power utilities, research institutes and universities have been carrying out a lot of studies on the voltage instability/collapse problem[1]. Several indicators/indices have been suggested by a number of authors as a measure of voltage stability and extreme loading point proximity[2~6]. The dynamic behavior of collapses has recently been analyzed by several authors [7~12], and some modifications to the conventional load flow method are proposed in a couple of papers[13, 14].

Most of the previous studies are not identical and considered systems under fixed loading/generation conditions, and the major part of methodologies is based basically on the conventional load flow method and Jacobian matrix of power flow equation or $P-V$ curves. Since most of the voltage instability/collapse problem becomes problematic mainly under the heavily loaded conditions or ill-conditions of power systems, computational difficulties due to ill-conditions often occur when obtaining the power flow solution near the maximum loading point using the conventional load flow solution method. The cause of this difficulty is known to be the coincidence of extreme loading point with the singular point in load flow solution.

The paper presents an effective approach for calculating the extreme loading point and the upper side of the nose curves in order to provide detail and visual information of the voltage profile of power systems to operators and planners. In this paper, a modified load flow calculation method for ill-conditioned power systems[15] is introduced for the purpose of seeking more precise load flow solutions and the upper side of the nose curves. The Continuation Method[13, 16] is also used as a part of the solution algorithm for the calculation of extreme loading point and nose curves. The conventional polar coordinate based $N-R$ load flow program is modified to avoid numerical difficulties caused by the singularity of the Jacobian matrix occurring in the vicinity of the extreme loading point of heavily loaded systems.

The effectiveness of the proposed approach has been demonstrated by applying it to several sample power systems.

2. Modification of $N-R$ load flow method

2.1 Derivation of the optimal multiplier for polar coordinates formulation

A load flow calculation method for ill-conditioned power systems proposed in the paper[15], but it is described in rectangular coordinates and it can be changed in polar coordinates as follows (See the reference for the details).

$$y_s - y(x^r) - \mu J^r \Delta x^r - \mu^2 y(\Delta x^r) = 0 \quad (1)$$

$$y_s - y(x^p) - \mu J^r \Delta x^r - \mu^2 y(\Delta x^p) = 0 \tag{2}$$

where,

r : denotes rectangular coordinate quantities

p : denotes polar coordinate quantities

The second and the fourth terms of equation (1) and (2) are the same, and the third term can be expressed approximately as

$$J^r \Delta x^r \cong J^p \Delta x^p + J^p \Delta \Delta x^p \tag{3}$$

where, $\Delta \Delta x^p = 1/2 [dx^p / dx^r ((\Delta x^p)^t d^2 x^r / (dx^p)^2 \cdot \Delta x^p)]$

Consider that the vector x^p has the form in polar coordinates load flow equation as

$$(x^p)^t = [\delta_i |E_i| \delta_2 \dots] \tag{4}$$

The $\Delta \Delta x^p$ term can be determined to be

$$(\Delta \Delta x^p)^t = [\Delta \delta_i \Delta |E_i| / |E_i|, -|E_i| \Delta \delta_i^2 / 2, \Delta \delta_2 \Delta |E_2| / |E_2|, -|E_2| \Delta \delta_2^2 / 2 \dots] \tag{5}$$

Which is a vector with a simple structure. Thus all the terms in equation (2) can be evaluated, and the same procedure described in (7) ~ (12) of the reference [15] can be used to find the optimal multiplier μ . Once μ is found it can be used as in the paper [15], to manipulate the step size Δx .

2.2 Application of the optimal multiplier to the polar coordinates N-R method

In the N-R method, the correction vector Δx^p is obtained basically by triangulating the Jacobian matrix in the following equation.

$$J \Delta x^p = y_s - y(x_e^p) \tag{6}$$

where,

x_e : estimate of x

J : Jacobian matrix

Δx : correction vector

From equation (2), (3) and (6), the following relationships are obtained.

$$a = [a_1, \dots, a_n]^t = y_s - y(x_e^p) \tag{7}$$

$$b = [b_1, \dots, b_n]^t = -J^r \Delta x^r = -J^p \Delta x^p - J^p \Delta \Delta x^p = -a^p - J^p \Delta \Delta x^p \tag{8}$$

$$c = [c_1, \dots, c_n]^t = -y(\Delta x^p) \tag{9}$$

Then, equation (2) can be written simply as below

$$a + \mu b + \mu^2 c = 0 \tag{10}$$

In order to determine the value of μ in a least squared sense, the following cost function is considered.

$$\text{Minimize : } F = 1/2 \sum (a_i + \mu b_i + \mu^2 c_i)^2 \tag{11}$$

The optimal solution μ^* of the above equation can be obtained by solving the equation below.

$$\partial F / \partial \mu = 0 \tag{12}$$

Namely,

$$g_0 + g_1 \mu + g_2 \mu^2 + g_3 \mu^3 = 0 \tag{13}$$

where,

$$g_0 = \sum (a_i b_i), g_1 = \sum (b_i^2 + 2 a_i c_i) \\ g_2 = 3 \sum (b_i c_i), g_3 = 2 \sum c_i^2 \tag{14}$$

The above equation can be solved easily using the IMSL library, and application procedures of the optimal multiplier, which is introduced in order to manipulate the size of correction vector in this paper, are as follows.

- 1) Start the conventional polar coordinate N-R load flow calculation
- 2) Compute Δx^p by conventional N-R method
- 3) Compute a , b and c using equations (7) ~ (9)
- 4) Compute g_0 , g_1 , g_2 and g_3 using equation (14)
- 5) Equation (13) will be solved using IMSL library to calculate μ^*
- 6) Manipulate the correction vector as follows $\Delta x^p = \mu^* \cdot \Delta x^p$
- 7) Update the variables $x^{p(n+1)} = x^{p(n)} + \Delta x^p$
- 8) Proceed the same step as conventional N-R load flow method

2.3 Application results and recommendations

In order to assure the feasibility of the modified N-R load flow method to the calculation of extreme loading point and nose curves, study cases were performed on several power systems and the following results were obtained.

- 1) Klos-Kerner (K&K) 11-bus system
 - a) More precise solutions were obtained
 - + P-Mismatch = -0.46 [MW],
 - Q-Mismatch = -3.91 [MVar]
 - * P-Mismatch = -0.03 [MW],

$$Q\text{-Mismatch} = -0.27 [\text{MVar}]$$

b) Number of iterations is increased by 3 (from 8 to 11)

2) B39M(modified IEEE 30-bus) system
The mismatch and the number of iteration counts are the same in this case.

3) IEEE 118-bus system

a) The mismatch become slightly bigger

$$+ P\text{-Mismatch} = 0.0 [\text{MW}],$$

$$Q\text{-Mismatch} = 0.0 [\text{MVar}]$$

$$* P\text{-Mismatch} = -0.89 [\text{MW}],$$

$$Q\text{-Mismatch} = -1.70 [\text{MVar}]$$

b) Number of iterations is decreased by 1 (from 6 to 5)

4) TX 1879-bus system (Texas 1879-bus actual power system)

a) P mismatch is the same and Q -mismatch is slightly decreased

$$+ P\text{-Mismatch} = 0.01 [\text{MW}],$$

$$Q\text{-Mismatch} = -0.42 [\text{MVar}]$$

$$* P\text{-Mismatch} = -0.01 [\text{MW}],$$

$$Q\text{-Mismatch} = -0.19 [\text{MVar}]$$

b) Number of iterations is decreased by 6 (from 18 to 12)

In the above summary, +, * denote the results before and after application of the optimal multiplier respectively, and the detail explanation on the value of optimal multiplier and the its application effects are summarized in Table 1 and Fig. 1,

From the test results ;

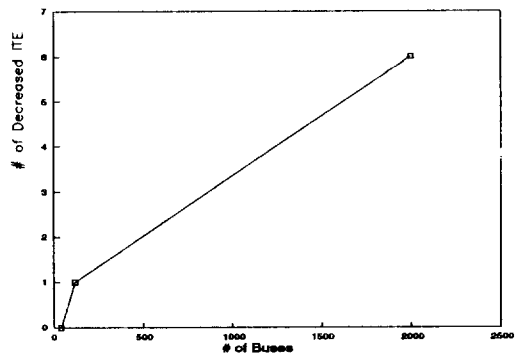


Fig. 1 Comparison between # of buses and iterations

- 1) The above mentioned modification is very useful from the practical point of view.
- 2) The method can be used as a detection indicator of the existence of the load flow solution using the characteristic of optimal multiplier. It goes to zero rapidly in the case of no existing solution, and it has the value of around 1.0 when there is a solution within several iterations. Therefore, we do not need to wait until it diverges in case of no existing solution.
- 3) The larger the system size becomes, the more the number of iterations decrease.
- 4) In the case that a system is heavily loaded, a more precise solution will be obtained (refer

Table 1 Summary of Optimal Multiplier

ITE	K&K (A)	K&K (B)	B30M (A)	B30M (B)	IEEE118 (A)	TX1879 (A)
1	0.76907	0.66018	0.95602	0.70888	0.90565	0.91521
2	0.80724	0.39952	1.00736	0.62581	0.91755	0.90298
3	0.76749	0.04411	0.99909	0.29690	1.05945	1.00355
4	0.75424	0.00852	1.00000	0.00013	0.99396	0.96547
5	0.76309	0.00264		0.00000	0.99877	0.99912
6	0.78297	0.00094				0.99791
7	0.81221	0.00036				0.94758
8	0.85916	0.00014				0.99571
9	0.92942	0.00006				0.92967
10	0.98571	0.00001				0.99823
11	0.99955	0.00000				0.98009
12						0.99997

(A) : convergent case, (B) : divergent case

to study results of Klos-Kerner system).

- 5) This method gives a solution which is very close to the extreme loading point but it is not the exact point. So it is not enough to apply this method for the calculation of extreme loading point and nose curves.
- 6) Since the modified method can be easily incorporated into the conventional $N-R$ load flow program (in rectangular/or polar coordinates), all current load flow programs should be modified to incorporate the use of this technique in order to obtain a more precise solution and decrease the number of iteration counts.
- 7) This method will be used as a basic tool for the calculation of extreme loading point and nose curves in this study.

3. Calculation of extreme loading point and nose curves

3.1 Formulation of the problem using the Continuation Method

The loading/generation scenario from operating point to extreme point is indispensable in this approach, and the basic assumptions are as follows.

- 1) The power factor at each bus is kept constant independently of load demand or the active power of load.
- 2) The load demand at each bus is increased at the same rate from the base load.
- 3) The active power output of each generator is also increased at the same rate except at the slack bus, the increment of transmission loss is absorbed by the slack generator.
- 4) The magnitude of generator bus voltage is kept constant within its regulating limits, and after violation of the limits the bus is changed to $P-Q$ bus.
- 5) The increasing rate will be determined by the autoscaling factor " α ".

According to the above mentioned loading/generation scenario from a base load to an extreme load, the load/generation increasing formula is defined as follows.

$$Y_s(t) = Y_{s0} + tY_d \tag{15}$$

where,

Y_{s0} : specified value of base load and generation

Y_d : loading/generation pattern

t : scalar parameter (increasing rate)

$Y_d = [\Delta P_g, \Delta P_l, \Delta Q_l]^T$ is arbitrarily selected.

The scalar parameter t is a scale of demand growth which is used as the horizontal axis in the nose curves.

By substituting equation (15) the load flow equation, an augmented equation as (16) is obtained.

$$\begin{aligned} H(x, t) &= Y(x) - Y_s(t) \\ &= Y(x) - Y_{s0} - tY_d = 0 \end{aligned} \tag{16}$$

The solution of $H(x, t) = 0$ also provides a load flow solution for specified value $Y_s(t)$. To estimate a solution $(x_0 + \Delta x, t_0 + \Delta t)$ that adjoins a known solution (x_0, t_0) , the linearized relations between Δx and Δt should satisfy following equation.

$$\begin{aligned} H(x_0 + \Delta x, t_0 + \Delta t) &= H(x_0, t_0) \\ &+ \partial H / \partial x \cdot \Delta x + \partial H / \partial t \cdot \Delta t = 0 \end{aligned} \tag{17}$$

In order for the above equation to be completed, the following relationship must be satisfied.

$$\partial H / \partial x \cdot \Delta x + \partial H / \partial t \cdot \Delta t = 0 \tag{18}$$

From equations (16) and (18)

$$J \Delta x - Y_d \Delta t = 0 \tag{19}$$

It might be a good idea to solve the conventional load flow problem by setting the specified value $Y_s = Y_s(t_0 + \Delta t)$ and the initial condition $x_0 = x_0 + \Delta x$. It is not enough, however, to overcome the numerical difficulties near the extreme loading point. In this paper, the Continuation Method is introduced to avoid the difficulties.

Generally, the load flow equation of power systems is represented by nonlinear simultaneous equation.

$$f(x) = 0 \tag{20}$$

It is solved by Newton like methods starting from an arbitrarily selected initial value x_0 , and the convergency properties are not always guaranteed.

Under the premise that equation (20) will be satisfied eventually, $(n-1)$ equations are embed-

ded between the equation whose obvious solution is known and the equation (20) which should be solved, the series of solutions will be obtained gradually.

For example, an equation corollary

$$f(x) = f(x_0) \tag{21}$$

has a solution $a(0) = x_0$, where $a(0)$ means an obvious solution which is determined by a physically reasonable starting point x_0 (it will be one of the load flow solution in this paper). Let's consider an equation corollary which has t as a parameter:

$$f(x) - (1-t)f(x_0) = 0 \tag{22}$$

In the above equation, if $t=0$, it is the same as equation (21), and when $t=1$, it will be the same as equation (20). Let the solutions for various $t=1/n, 2/n, \dots, (n-1)/n$ and 1 be $a(1/n), a(2/n), \dots, a((n-1)/n)$ and $a(1)$, the $a(1)$ is the very desired solution. So the solutions of the equation for $t=m/n$ and the equation for $t=(m+1)/n$, $a(m/n)$ and $a((m+1)/n)$ are very closely located that the solution $a((m+1)/n)$ is easily obtained using Newton like methods starting from $a(m/n)$. The purpose of this equation is to trace a curve of solutions from an arbitrary initial condition x_0 at $t=0$ to a desired solution x at $t=1$. In this paper, however, $t=1$ has no special meaning and it will be substituted for the extreme loading points of the systems.

The Continuation Method is generalized as follows based on the concepts mentioned above, For the purpose of brief description of the Continuation Method (refer to reference [16] for the details), besides equation (20), another equation of which a solution is known will be defined as (23).

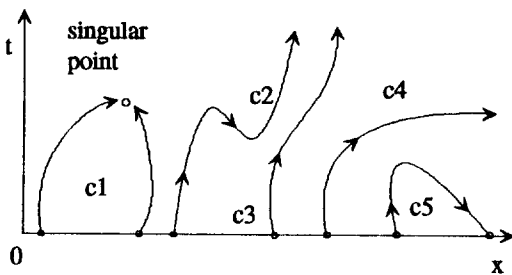


Fig. 2 Several curves of $h(x, t) = 0$

$$g(x) = 0 \tag{23}$$

The equation (23) is the solution of the base load condition and will be the starting point of the continuation method. Let's consider a function which connects between f and g successively and has $(n+1)$ variables.

$$\begin{aligned} h(x, t) &= 0, t \in [0, 1] \\ h(x, 0) &= g(x), h(x, 1) = f(x) \end{aligned} \tag{24}$$

The points which satisfy the equation (24) in the space (x, t) is able to produce several continuous curves like Fig. 2.

From equation (24), a differential equation of the curves is

$$H_0(x, t) dt/ds + \sum H_j(x, t) dx_j/ds = 0 \tag{25}$$

where,

s : parameter along the curves, and the solution point on the curve will be described as $x(s), t(s)$.

$$H_0(x, t) = \partial h(x, t) / \partial t, H_j(x, t) = \partial h(x, t) / \partial x_j$$

and a condition, for example.

$$(dt/ds)^2 + \sum (dx_j/ds)^2 = 1 \tag{26}$$

may be imposed for the purpose of finding the solution which exists on the curve (see the Fig. 3). The value 1 in the equation has no particular meaning and it can be selected arbitrarily as " k " in equation (28). The solution procedure of equation (24) is as follows.

- 1) Set $x(0) = x_0, t(0) = 0$ using the solution of $g(x) = 0$
- 2) If $x(s)$ and $t(s)$ are known, $x(s + \Delta s)$ and $t(s + \Delta s)$ will be determined using equations

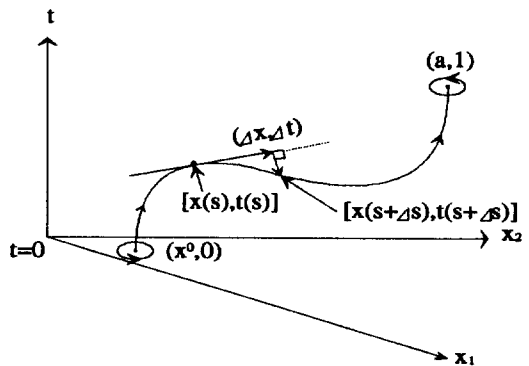


Fig. 3 Concept of the Continuation Method

below.

$$H_0(x(s), t(s))\Delta t + \sum H_j(x(s), t(s))\Delta x_j = 0 \quad (27)$$

$$(\Delta t)^2 + \sum (\Delta x_j)^2 = (\Delta s)^2 = k \quad (28)$$

The condition described in the above equation correspond to the condition of (26). The value of k should be selected manually to limit size of the vector $(\Delta x, \Delta t)$. If k is greater than the region in which the linearization is valid, numerical instabilities may appear in the later process. Conversely, if k is set to a small value, the size of the step toward the extreme point is small. The k is constant from $t=0$ through $t=t_{max}$ along the locus of $H(x, t)=0$. The step size Δt , however, varies automatically during the iterative process to satisfy equation (28).

- 3) The solution point $(x(s)+\Delta x, t(s)+\Delta t)$ is not exactly on the curve but in the vicinity of the curve. Thus, solve the following two equations simultaneously by the Newton-Raphson method and the desired solution is finally obtained.

$$h(x(s+\Delta s), t(s+\Delta s))=0 \quad (29)$$

$$\Delta t[t(s+\Delta s)-(t(s)+\Delta t)] + \sum \Delta x_j [x_j(s+\Delta s)-(x_j(s)+\Delta x_j)]=0 \quad (30)$$

Equation (30) means the hyperplane that is perpendicular to the vector $(\Delta x, \Delta t)$, and also crosses at $(x(s)+\Delta x, t(s)+\Delta t)$. Fig. 3 illustrates this concept. The size of the Jacobian matrix of this problem is larger than that of the conventional load flow problem by only one dimension as shown in equation (31).

$$J_h = \begin{bmatrix} J(x) & -Y_d \\ \Delta x & \Delta t \end{bmatrix} \quad (31)$$

3.2 Calculation procedures of the extreme loading point and nose curves

In order to avoid the instability caused by the relatively light loaded condition of a system, the original method for calculation of extreme loading points [15] is modified to incorporate the modified $N-R$ load flow method. Using the proposed method, the solution procedure is very stable and feasible solutions are obtained always regardless of the loading situation of the power systems.

Calculation procedures of the proposed method

are as follows.

- step1) Solve a load flow problem to obtain the solutions $x(V, \theta)$ for the base load condition ($t=0$) using the modified (optimal multiplier introduced) $N-R$ load flow method.

- step2) Set loading/generation pattern Y_d and power factor of the system according to the operation guidance, and select an appropriate value of the parameter " k " (k_1 & k_2).

- step3) Calculate Δt using equation (32) ~ (34).

$$\Delta z_i = J^{-1} Y_d \quad (32)$$

$$\alpha = [k_1 / \sum \Delta z_i^2]^{1/2} \quad (33)$$

$$\Delta t = \alpha \quad (34)$$

- step4) Increase loading/generation value using the scenario and Δt .

- step5) Solve the load flow problem by the modified polar coordinate based $N-R$ method and store the intermediate solution $(x(s+\Delta s), t(s+\Delta s))$, and update x and t .

- step6) If the solution is obtained successfully, go back to step 3. Otherwise, that is, once divergency is occurred at the vicinity of extreme loading points, go to the next step (switch the solution routine to the Continuation Method).

- step7) Calculate Δx and Δt using equation (35) ~ (38).

$$\Delta z_i = J^{-1} Y_d \quad (35)$$

$$\alpha = [k_2 / \sum \Delta z_i^2]^{1/2} \quad (36)$$

$$\Delta x_i = \Delta z_i \cdot \alpha \quad (37)$$

$$\Delta t = \alpha \quad (38)$$

- step8) Solve equations (29) and (30) by the conventional $N-R$ method using $x, t, \Delta x$ and Δt . The exact solution $(x(s+\Delta s), t(s+\Delta s))$ will be obtained.

- step9) Store the intermediate solution $(x(s+\Delta s), t(s+\Delta s))$, and update x and t .

- step10) If $\Delta t > \epsilon$, go back to step 7. Otherwise stop. The terminal point $Y_s(t)$ is the extreme loading point and the nose curves will be drawn using the intermediate solutions.

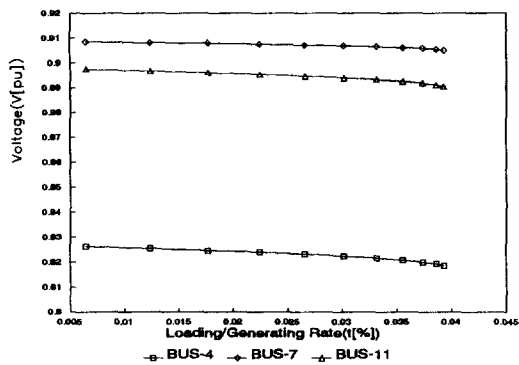


Fig. 4 Upper side of nose curves of Klos-Kerner system

4. Study cases and results

This effectiveness of the proposed approach has been demonstrated by applying it to several sample power systems. The study cases and results are as follows.

4.1 Klos-Kerner(K&K) 11-bus system

This sample system is well known as a heavily loaded system.

1) Set system conditions

$$Y_d = 1.0 \cdot L_d, \text{ where } L_d \text{ is system base load}$$

$$\text{Power factor} = 0.98$$

2) Selection of the parameter "k"

$$k_1 = 0.01, k_2 = 0.001$$

Fig. 4 shows the extreme loading point and the upper side of nose curves of the K&K 11-bus system and the buses are selected arbitrarily in

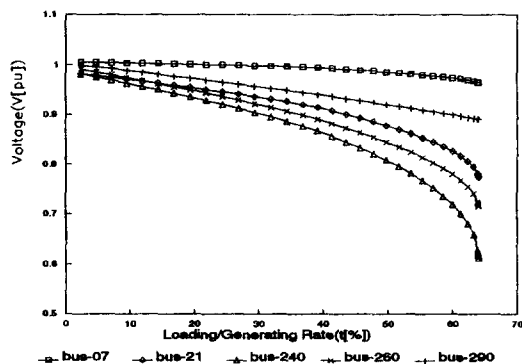


Fig. 5 Upper side of nose curves of B39M system

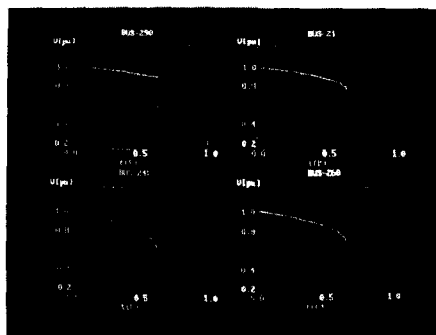


Fig. 6 A picture of the visual information from graphic monitor (I)

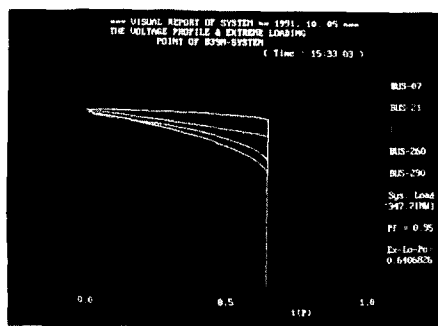


Fig. 7 A picture of the visual information from graphic monitor (II)

Table 2 Upper side information of nose curves of K&K 11-bus system

No.	t (%)	dt	BUS-04	BUS-07	BUS-11
1	.0000000	.0000000	.8264123	.9088123	.8996321
2	.0064783	.0000648	.8263413	.9086172	.8976016
3	.0123749	.0000590	.8255628	.9082732	.8968924
4	.0176900	.0000532	.8247836	.9079297	.8961824
5	.0224239	.0000473	.8240038	.9075867	.8954716
6	.0265764	.0000415	.8232233	.9072442	.8947599
7	.0301477	.0000357	.8224421	.9069022	.8940474
8	.0331380	.0000299	.8216603	.9065607	.8933340
9	.0355472	.0000241	.8208778	.9062197	.8926199
10	.0373756	.0000183	.8200946	.9058791	.8919050
11	.0386231	.0000125	.8193108	.9055392	.8911892
12	.0392900	.0000067	.8185264	.9051996	.8904725

this test example.

Power factor=0.95

2) Selection of the parameter "k"

$k_1=0.005, k_2=0.001$

4.2 B39M(Modified IEEE 30-bus) system

1) Set system conditions

$Y_d=1.0 \cdot L_d$, where L_d is system base load

Fig. 5 shows the extreme loading point and the upper side of nose curves of the B39M system and

Table 3 Upper side information of nose curves of B39M system

No.	t (%)	BUS-7	BUS-21	BUS-240	BUS-260	BUS-290
1	0.000000	1.0063212	.9834342	.9823213	.9917625	.9998231
2	2.3256900	1.0061390	.9832041	.9821303	.9915503	.9996069
3	4.6859260	1.0055270	.9795998	.9761868	.9861901	.9961879
4	7.0716500	1.0049000	.9758763	.9700388	.9806595	.9926881
5	9.4810600	1.0042570	.9720333	.9636812	.9749535	.9891070
6	11.9121800	1.0035980	.9680652	.9571044	.9690663	.9854456
7	14.3628400	1.0029240	.9639692	.9503015	.9629931	.9817030
8	16.8306700	1.0022340	.9597402	.9432611	.9567256	.9778811
9	19.3130700	1.0015280	.9553744	.9359744	.9502584	.9739801
10	21.8072300	1.0008060	.9508694	.9284333	.9435858	.9700021
11	24.3100900	1.0000690	.9462173	.9206226	.9366984	.9659489
12	26.8183000	.9993154	.9414160	.9125329	.9295903	.9618227
13	29.3282600	.9985465	.9364597	.9041504	.9222518	.9576271
14	31.8360700	.9977619	.9313423	.8954598	.9146748	.9533660
15	34.3374600	.9969617	.9260612	.8864487	.9068513	.9490438
16	36.8278500	.9960078	.9203740	.8768488	.8986546	.9446660
17	39.1000000	.9946837	.9142519	.8669204	.8905191	.9406047
18	41.3379400	.9929962	.9073631	.8560065	.8818532	.9365388
19	43.5318900	.9912814	.9002786	.8447020	.8729430	.9324872
20	45.6754000	.9895391	.8929850	.8329747	.8637763	.9284635
21	47.7414600	.9877716	.8854837	.8208064	.8543502	.9244827
22	49.7825900	.9859794	.8777639	.8081604	.8446528	.9205619
23	51.7306000	.9841630	.8698156	.7949961	.8436725	.9167219
24	53.5965000	.9823232	.8616263	.7812639	.8243957	.9129844
25	55.3702900	.9804621	.8531877	.7669103	.8138112	.9093759
26	57.0407500	.9785795	.8444774	.7518517	.8028958	.9059260
27	58.5949700	.9765750	.8354707	.7359866	.7916260	.9026690
28	60.0177500	.9747468	.8261236	.7191573	.7799584	.8996467
29	61.2905300	.9727904	.8163754	.7011408	.7678324	.8969090
30	62.3896400	.9707913	.8060905	.6815196	.7551146	.8945183
31	63.2823900	.9687022	.7949187	.6593334	.7414386	.8925571
32	63.9164700	.9661835	.7807000	.6293725	.7243816	.8911539
33	63.9626400	.9659729	.7794623	.6266586	.7229219	.8910928
34	64.0007600	.9657929	.7782214	.6239174	.7214636	.8910424
35	64.0306300	.9655537	.7769771	.6211481	.7200068	.8910029
36	64.0519900	.9653453	.7757296	.6183499	.7185521	.8909746
37	64.0646300	.9651376	.7744789	.6155216	.7170997	.8909580
38	64.0682600	.9649308	.7732249	.6126624	.7156501	.8909531

the buses are also selected arbitrarily in this test example.

The numerical outputs are summarized in Table 2 and Table 3 respectively, and Fig. 6 and Fig. 7 are some picture examples of visual information which will be provided to operators/planners of power systems through on-line color graphic monitor.

5. Conclusions

This paper presents an effective approach for calculating the extreme loading point and the upper side of nose curves in order to provide detail and visual information on the voltage profile of power systems to operators and planners.

The obtained conclusions are as follows.

- 1) The modified $N-R$ load flow calculation method for ill-conditioned power systems is introduced for the purpose of seeking more precise load flow solutions and the upper side information of nose curves, that is, the conventional polar coordinate based $N-R$ load flow program is modified to avoid numerical difficulties caused by the singularity of the Jacobian matrix occurring in the vicinity of the extreme loading point of heavily loaded power systems.
- 2) The obtained results are not only more precise but also the larger the system size becomes, the more the number of iterations decrease, which is very interesting and unexpected but beneficial phenomenon.
- 3) The method can be used as a detection indicator of load flow solution existence using the characteristic of optimal multiplier, and it is used as a basic tool for the calculation of extreme loading point and nose curves.
- 4) The Continuation Method is also used as a part of the solution algorithm to obtain the exact solution of extreme loading point and nose curves.
- 5) The critical loading point and the nose curves obtained by the method will be very useful information to power system operators and planners, and the visual information can be used as an important message crea-

tion tool of Operator Training Simulator (OTS).

- 6) The proposed method can be used as a tool for an on-line voltage security monitoring systems.
- 7) The information on the extreme loading point and voltage profile might be applied to Automatic Generation Control Simulator (AGCS) through the appropriate feedback procedure. This is a field for further study.

REFERENCES

- [1] EPRI Report, "Bulk Power System Voltage Phenomena-Voltage Stability and Security," EPRI EL-6183, Project 2473-21, 1989
- [2] Y. Tamura, et al, "Relationship between Voltage Instability and Multiple Load Flow Solutions in Electric Power Systems," IEEE Trans. on PAS, Vol. PAS-102, No. 5, 1983
- [3] K.P. Kessel, et al, "Estimating the Voltage Stability of a Power System," IEEE Trans. on PWRD, Vol. PWRD-1, No. 3, 1986
- [4] R.J. Thomas, et al, "Posturing Strategy Against Voltage Instabilities in Electric Power Systems," IEEE Trans. on PWRD, Vol. PWRD-3, No. 5, 1988
- [5] A. Semlyem, et al, "Calculation of the Extreme Loading Condition of a Power System for the Assessment of Voltage Stability," IEEE Trans. on PWRD, Vol. PWRD-6, No. 1, 1991
- [6] G. Anderson, "Fast Calculation of a Voltage Stability Index," IEEE Winter Meeting Paper, 91 WM203-0, 1991
- [7] J. Medanic, et al, "Discrete Models of Slow Voltage Dynamics for Under Load Tap Changing Transformer Coordination," IEEE Trans. on PWRD, Vol. PWRD-2, No. 4, 1987
- [8] C.C. Liu, et al, "Analysis of Tap Changer Dynamics and Construction of Voltage Stability Regions," IEEE Trans. on Circuits and Systems, Vol. 36, 1989
- [9] H.D. Chiang, et al, "On Voltage Collapse in Electric Power Systems," IEEE Trans. on PWRD, Vol. PWRD-5, No. 2, 1990
- [10] Y. Sekine, et al, "Cascaed Voltage Col-

- lapse," IEEE Trans. on PWRS, Vol. PWRS-5, No. 1, 1990
- [11] Y. Tamura, et al, "An Investigation of Voltage Instability Problems," IEEE Winter Meeting Paper, 91 WM202-2, 1991
- [12] K.Y. Lee, et al, "A Study on the Voltage Collapse Mechanism in Electric Power Systems," IEEE Winter Meeting Paper, 91 WM-123, 1991
- [13] K. Iba, et al, "Calculation of Critical Loading Condition with Nose Curve using Homotopy Continuation Method," IEEE Trans. on PWRS, Vol. PWRS-6, No. 2, 1991
- [14] Y. Kataoka, "An Approach for the Regularization of a Power Flow Solutions Around the Maximum Loading Point," IEEE Winter Meeting Paper, 91 WM099-2, 1991
- [15] S. Iwamoto, et al, "A Load Flow Calculation Method for ill-conditioned Power Systems," IEEE Trans. on PAS, Vol. PAS-100, No. 4, 1981
- [16] M. Tataeri, "Mumerical Calculation-Solution Methods of Equations," Asa-Kura Press, Japan, 1981

저 자 소 개



유인근(劉仁根)

1954년 2월 18일생. 1981년 동국대 공대 전기공학과 졸업. 1983년 한양대 대학원 전기공학과 졸업(석사). 1986년 동 대학원 전기공학과 졸업(공학). 1985~88년 한국전기연구소 선임연구원. 1990~91 미국 UTA Post-Doc. 연수. 현재 창원대 공대 전기공학과 조교수.